

DESIGN OF MULTIMODE WAVEGUIDE TRANSITION SECTIONS BASED ON RADIAL AND RECTANGULAR MODAL ANALYSES

E. Bahar and G. Govindarajan
 Electrical Engineering Department
 University of Nebraska
 Lincoln, Nebraska 68508

Abstract

Multimode waveguide transition sections are designed based on a quasi-optical approach and rectangular and radial modal analyses. The radial modal analysis is most suitable for large flare angle transitions possessing spurious mode cut-off cross-sections.

Summary

Waveguide transition sections used to connect waveguides that support only one propagating mode to multimode waveguides play an important role in the design of high powered microwave systems. In order to limit the use of mode filters in these systems, it is necessary to design transition sections with minimal spurious mode content at the output ports.¹ In other special cases (as for the excitation of multimode waveguides with an inhomogeneous dielectric filling) it is necessary to design transition sections with specific modal contents.² In all these cases it is necessary to determine the variable cross section of the transition section with the desired transmission properties.

Various methods have been used to determine the mode amplitudes in waveguides with nonuniform cross sections. A brief survey of the different techniques used has been presented earlier.³ In this paper we examine three different approaches used to derive the first-order coupled differential equations for the wave amplitudes in H-plane nonuniform waveguides with rectangular cross sections.

The first, solution (a), is derived by Schelkunoff,⁴ who employs a full wave approach to convert Maxwell's equations into "generalized telegraphist's equations for waveguides." In this analysis the transverse electromagnetic fields at any cross section normal to the axis of the nonuniform waveguide are expanded in terms of a complete set of waveguide modes for uniform rectangular waveguides.

The second, solution (b), employs a quasi-optical approach in which reflections are neglected at the outset and the maximum flare angles of the non-uniform waveguides are assumed to be less than 15°.¹ In this analysis the transverse fields in the transition section are expanded in terms of a complete set of waveguide modes for elementary radial waveguides and asymptotic expressions are used for the radial dependence of the fields. Thus all the spurious modes considered are also assumed to be propagating.

The third, solution (c), can be applied to analyze waveguide transition sections with large flare angles.³ The spurious modes may be either evanescent or propagating in different regions of the nonuniform waveguide. In this analysis a full wave approach is used and the transverse fields are expressed in terms of a complete set of radial waveguide modes. Thus reflections are not neglected at the outset and rigorous expressions for the radial dependence of the fields are retained.

While the mode amplitudes depend upon whether the rectangular or radial modal analysis is used, they are the same for regions of the waveguide where the flare angle vanishes since in these regions the two modal expansions of the fields merge. The coupled differential equations for the mode amplitudes are solved numerically using an iterative approach and the more rigorous Runge-Kutta method.⁵

For multimode waveguides transition sections with small flare angles all three solutions are shown to agree with the experimental results. However, solution (b) is simple to program and requires the least computer time to execute.

For waveguides with large flare angles only the full wave solutions (a) and (c) should be used. Of these two solutions it is shown that solution (c) is more efficient. The reasons for this are basically threefold. Firstly, the coupling coefficients are singular at the spurious mode cut-off cross section only when solution (a) is used. Secondly, the coupling coefficients are proportional to the gradient of the height of the cross section when solution (a) is used and they are proportional to the curvature of the cross-sectional height when solution (c) is used. Thirdly, the spurious modes are more tightly bunched about the incident mode when solution (c) is used.

Another method for deriving the mode coupling coefficients is based on the expression of Maxwell's equations in a "natural" coordinate system,⁶ but as indicated by the author of this technique, it fails in regions where the curvature of the cross-section height profile is negative. All the solutions considered in this paper are not subject to this restriction.

The H-plane transition sections considered are of rectangular cross section of uniform width $d < \lambda/2$ (λ is the free space wave length). The cross section of the nonuniform waveguide is symmetric about its axis, x . The half height of the input and output ports are $h_a = .342\lambda$ and $h_b = 3.81\lambda$ respectively. The length of the transition section is $L = 68.58\lambda$. The half height of the cross section $h(x)$ and its derivative are in general continuous functions of x . The particular profile chosen in this work is given by:

$$h(x) = \frac{h_a + h_b}{2} + \frac{h_a - h_b}{2} \cos\left(\pi \frac{\exp(\alpha x/L) - 1}{\exp(\alpha) - 1}\right), \quad 0 \leq x \leq L. \quad (1)$$

By varying the design parameter α in (1) the height profile can be made to change gradually from an abrupt height discontinuity at the input port ($\alpha \rightarrow -\infty$) to a sinusoid (on linear scale) for $\alpha = 0$ and finally into an abrupt height discontinuity at the output port ($\alpha \rightarrow \infty$). For finite values of α the flare angles at the input and output ports vanish since $h'(0) = h'(L) = 0$ (see Fig. 1). The experimental work was conducted at 9.00 GHz and due to mechanical constraints the range of the design parameter α is between 3.0 and -3.0.

The waveguide transition section is excited by a $TE_{1,0}$ mode of unit amplitude which is the only propagating mode at the input port. Thus, due to the symmetry of the height profile about the x axis, only $TE_{n,0}$ modes ($n=1,3,5,7\dots$) are excited in the non-uniform waveguide.

The transverse electric and magnetic field components E_z and H_y respectively, at any cross section normal to the x axis of the waveguide, are expressed as follows in terms of the forward and backward wave

amplitudes a_n and b_n respectively

$$E_z = \sum_n (a_n + b_n) \psi_n, \quad H_y = \sum_n Y_n (a_n - b_n) \psi_n \quad (2)$$

in which ψ_n is the nth mode basis function.³

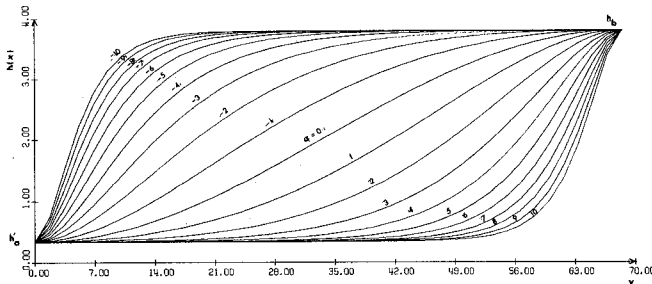
A detailed comparison of the numerical results obtained from the three different approaches discussed in this paper has been carried out.⁷

In Figures (2a) and (2b), solutions (a), (b) and (c) for the magnitude and phase of $a_3(L)/a_1(L)$ are plotted as a function of α ($-10 \leq \alpha \leq 10$) using the Runge-Kutta method. In Figures (3a) and (3b), the Runge-Kutta and the iterative approaches to solution (c) for the magnitude and phase of $a_3(L)/a_1(L)$ are compared with the corresponding experimental data.

References

1. E. Bahar and G. Crain, "Synthesis of Multimode Waveguide Transition Sections," Proc. IEE, Vol. 115, No. 10, pp. 1395-1397, 1968.
2. E. Bahar, "Inhomogeneous Dielectric Filling to Simulate Curvature in Model Earth-Ionosphere Waveguide," Proc. IEE, Vol. 116, No. 1, pp. 84-86, 1969.
3. E. Bahar, "Wave Scattering in Nonuniform Waveguides With Large Flare Angles and Near Cutoff," IEEE Transactions on Microwave Theory and Techniques, Vol. MTT-16, No. 8, pp. 503-510, 1968.
4. S. A. Schelkunoff, "Conversion of Maxwell's Equations into Generalized Telegraphist's Equations," Bell Sys. Tech. J., Vol. 34, pp. 995-1043, 1955.
5. M. Abramowitz and J. A. Stegun, Handbook of Mathematical Functions, National Bureau of Standards, Applied Mathematics Series 55, 1964.
6. H. G. Unger, "Wave Propagation in Horns and Through Horn Junctions," Arch. Elek. Übertragung, Vol. 19, pp. 459-468, 1965.
7. E. Bahar and G. Govindarajan, "H-Plane Waveguide Transition Sections With Large Flare Angles--Radial and Rectangular Modal Analyses," Proceedings IEE 1974 issue.

ILLUSTRATIONS



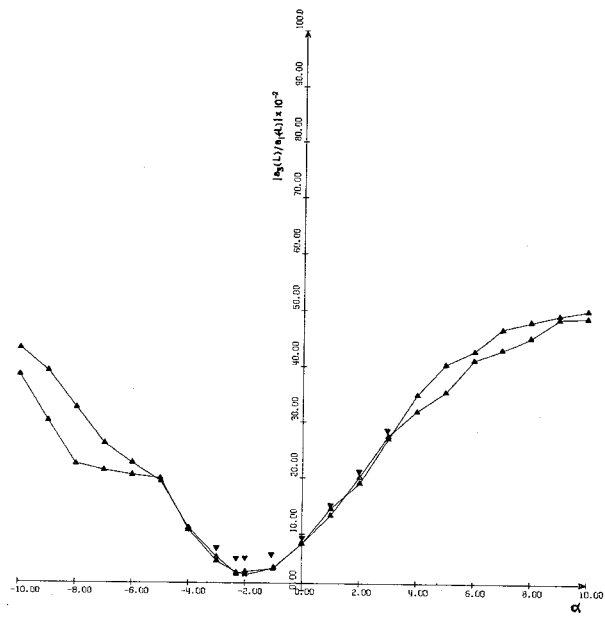


Fig. 3a Magnitude

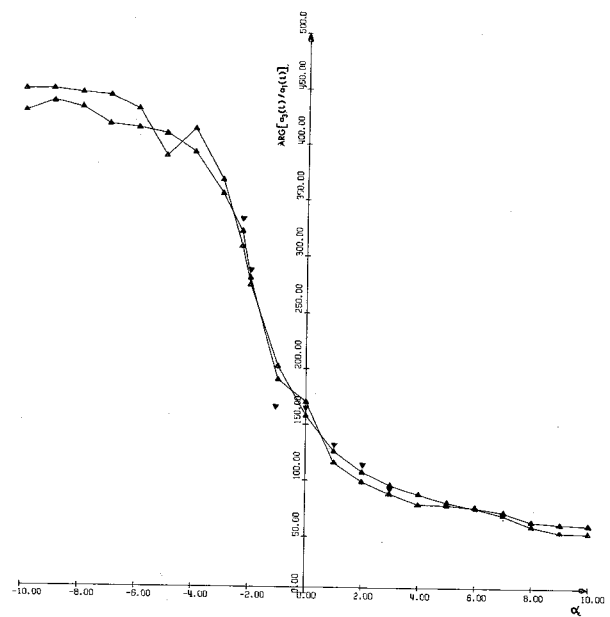


Fig. 3b Phase

Fig. 3 Comparison of full-wave solutions (c) with experimental data for $a_3(L)/a_1(L)$.

△ Runge-Kutta ▲ Iterative ▼ Experimental

Acknowledgments

This work has been supported by the National Science Foundation and the Engineering Research Center of the University of Nebraska.